Simulation of the Wind Performance of ASCAT

OSI SAF technical note

Ad Stoffelen - 1998

KNMI,
Postbus 201, 3730 AE de Bilt,
the Netherlands
E-mail: Ad.Stoffelen@knmi.nl

Abstract

In this note I use the ERS wind processing chain to simulate noisy backscatter values for ASCAT, retrieve winds from those, and compare them to the "true" wind. It is shown that, in order to achieve a constant performance versus across track node number, the instrument noise may be larger at the outer parts of the swath. This effect is quantified, and 25 versus 50 km resolution is investigated.

Introduction

For the design of the ASCAT scatterometer performance parameters have to be established. The ultimate goal of the scatterometer is to achieve a wind product with a specified quality. Given the ERS experience, detailed knowledge is available on the noise characteristics and performance of a C-band scatterometer such as ASCAT [1-4], that may be used to investigate the expected performance of it. ASCAT will have its swath extended to cover higher incidence angles, since the performance there would be better. This is confirmed here, but leaves us with a range of incidence angles for which the backscatter-to-wind transfer function has not been validated in the field. However, for the 7th ASCAT SAG meeting I made a presentation to show that the behaviour of CMOD4 [2] is rather smooth at the outer swath, and therefore one would not expect large errors by extrapolating CMOD4 to the outer ASCAT swath (see table 1 for incidence angles). Below, first the backscatter and backscatter noise simulation process is described, then the inversion to winds and evaluation of the performance. After presenting the results, suggestions will be presented on the specification of the instrument noise, and on the skill of high resolution wind scatterometry.

Simulation process

Figure 1 depicts the wind simulation chain. Here, sigma naught is abbreviated as s^0, Ng is geophysical noise, Kp instrumental noise, and a subscript $_S$ indicates a noisy value. PREASCAT is a modification of PRESCAT [4] that can handle the outer swath of ASCAT.

The winds we use as input are from the ECMWF. We decomposed the wind vector into a component along the swath pointing into the direction of satellite propagation, U, and a component pointing across the swath 90 degrees anti-clockwise from U, denoted V. Wind direction is according to the meteorological convention, which means that it is with reference to the V component direction, and measured clockwise. One and another is depicted in figure 2. We simulated only the right side of the ASCAT swath, since the performance on both sides is expected to be the same. This means that a direction upwind to the mid beam is always (0,V) with V 0. The distribution of ECMWF winds is the distribution obtained over the ERS-1 swath from 1 to 3 February 1996, and is thus realistic rather than theoretical. The winds serve as the truth reference in the statistics later on. The ASCAT nodes were simulated by 2nd order extrapolation from the 19 ERS nodes. As shown in table 1, I use the ERS numbering convention and the first ASCAT node has assigned number 7 and the last (outer) node number 25. In the statistics shown later on, we group every two next nodes together, except for node 25.

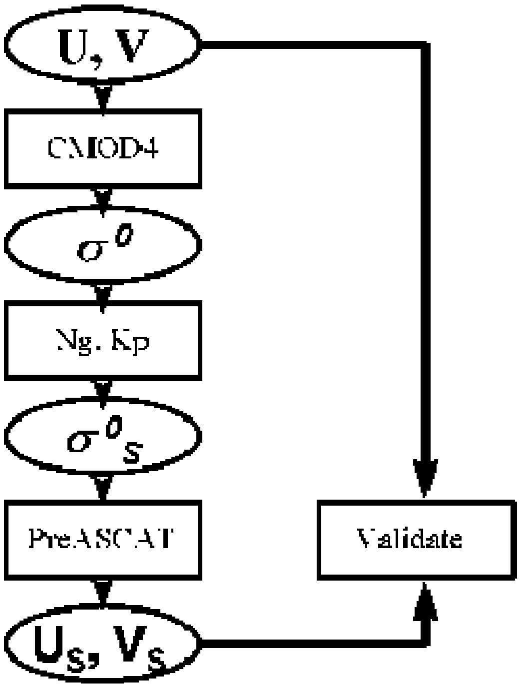

Figure 1: The ASCAT wind simulation chain (see text).

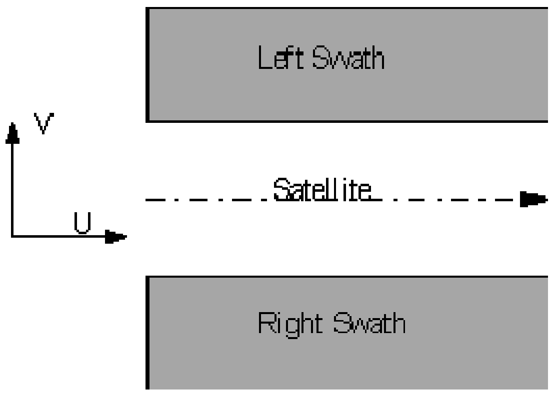

Figure 2: Definition of the wind.

Node	7	8	9	10	11	12	13	14	15	16	17	18	19	**20**	**21**	**22**	**23**	**24**	**25**
Fore	38.0	40.0	41.8	43.6	45.3	47.0	48.5	50.0	51.4	52.8	54.1	55.3	56.5	57.6	58.7	59.7	60.7	61.6	62.5
Aft	28.6	30.2	31.8	33.4	34.9	36.3	37.8	39.1	40.5	41.8	43.0	44.2	45.4	46.5	47.6	48.7	49.7	50.7	51.6

Table 1: Node numbering and incidence angles simulated for ASCAT. Note the ERS counting; new nodes for ASCAT are in bold.

As stated earlier CMOD4 was used to simulate "true" s^0 triplets from the "true" ECMWF winds. We assumed the presence of geophysical noise. Stoffelen and Anderson [1] quantified s^0 noise by investigating the distribution of s^0 triplets in the 3D measurement space. They find that the noise is 12%, 6%, and 5% at respectively 3, 9, and 16 m/s. So, in particular for low wind speeds the noise is larger than Kp = 5%, and they attributed this to additional geophysical noise. The geophysical noise is fitted as a fraction of s^0 by: $Ng(S) = 0.0644 (S - 16.)^2$ where S is wind speed. In addition to geophysical noise I simulated different levels of instrument noise, i.e. Kp = 0%, Kp = 5%, Kp = 10%, and Kp = 15 %. Geophysical and instrumental noise are squared, added, and taken the square root of, in order to compute the total Standard Deviation of Error (SDE). The SDE is multiplied by a random number, picked from a normal distribution with zero mean and a SD of one. The noisy triplets are processed by PREASCAT that has been modified from PRESCAT [1-4] in order to be able to handle the extended ASCAT swath. The procedure intelligently seeks the optimal wind speed and wind direction in a measurement domain that is defined by a Look-Up-Table, LUT. The LUT has a resolution of 1 degree in incidence angle, but s^0's are linearly interpolated in between. The wind speed and direction resolutions are 0.5 m/s and 5 degrees respectively. For a random sampling one would then expect a SDE of 0.15 m/s and 1.5 degrees in speed and direction respectively, due to the discretisation of the LUT.

Results

Figure 3 shows the general performance of several noise scenarii versus node number. All s^0 were inverted and no data loss occurred due to s^0 triplet Quality Control [2]. As a result the data represented in the statistics are virtually the same for all scenarii. The behaviour as a function of node number is rather smooth, indicating that the number of data used in the simulation is sufficient (close to 2000 per node). Figure 3 clearly shows that for a given s^0 noise, the performance increases with node number.

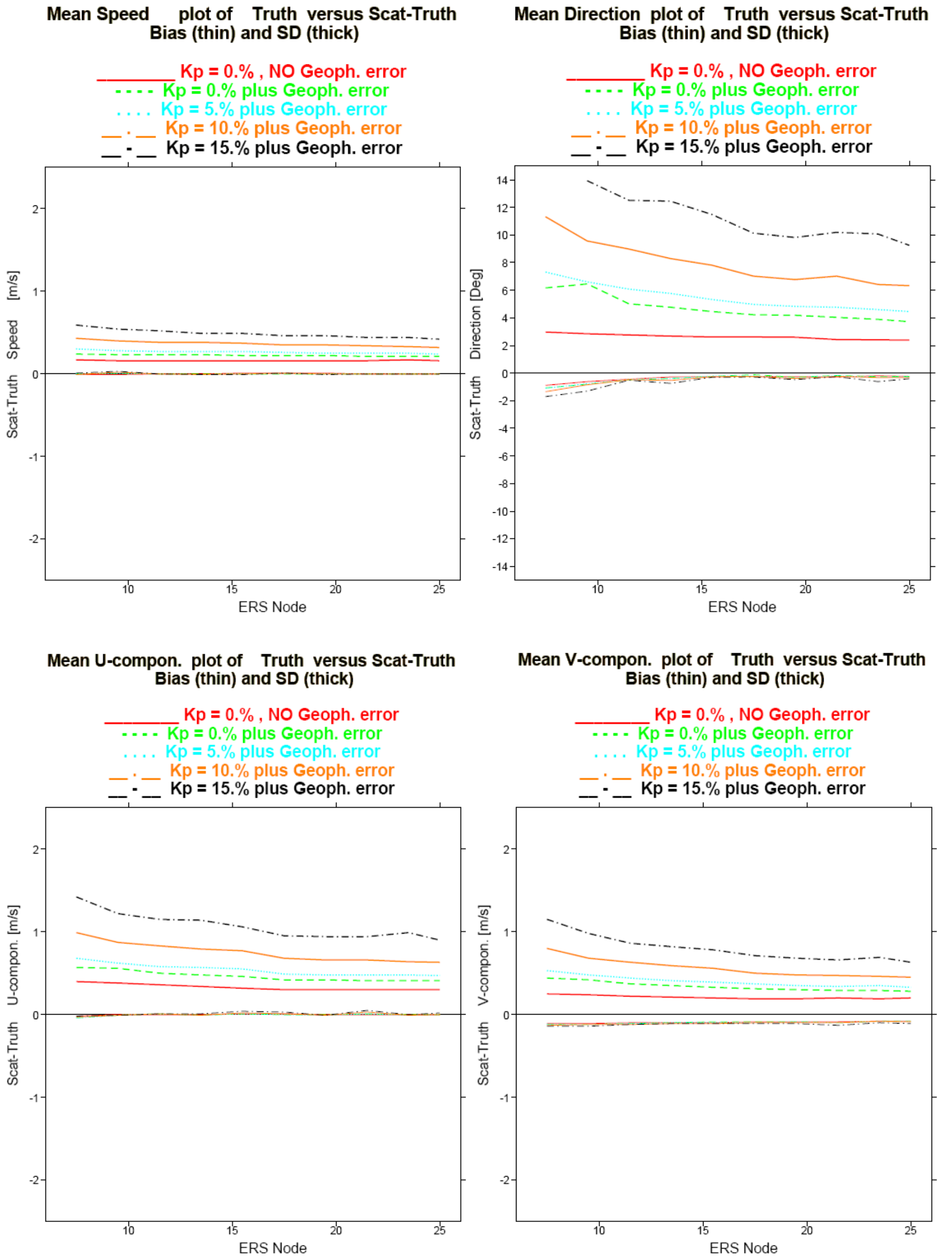

Figure 3: General performance of noise scenarii versus node number.

Figure 4 goes into more detail and shows the bias and SDE as a function of true wind speed, wind direction and wind components for each node set. Although the performance is node dependent, Figure 4 shows that the change of error with s^0 noise level, and the error versus true wind, is very similar for all nodes. Let us first focus on the performance without any noise on s^0. Ideally one would expect that the "true" wind and the wind retrieved from the "true" s^0 triplets were identical. However, the LUT approach may generate small errors. This turns out to be the case, and for wind direction slightly more than one would theoretically expect. This may be due to the strong non-linear behaviour at low wind speeds. Moreover, it turns out that the inversion causes a bias of ~0.1 m/s in the V component of the wind and this bias occurs irrespective of the s^0 noise. Closer inspection of this bias in Figure 4 shows that it is present for all V component magnitudes, and in wind direction a corresponding small negative bias is present for directions between 0 and 180 degrees, and a positive one from 180 to 360 degrees. Although this bias is small, it is of interest to investigate whether it is removed by increasing the resolution of the LUT.

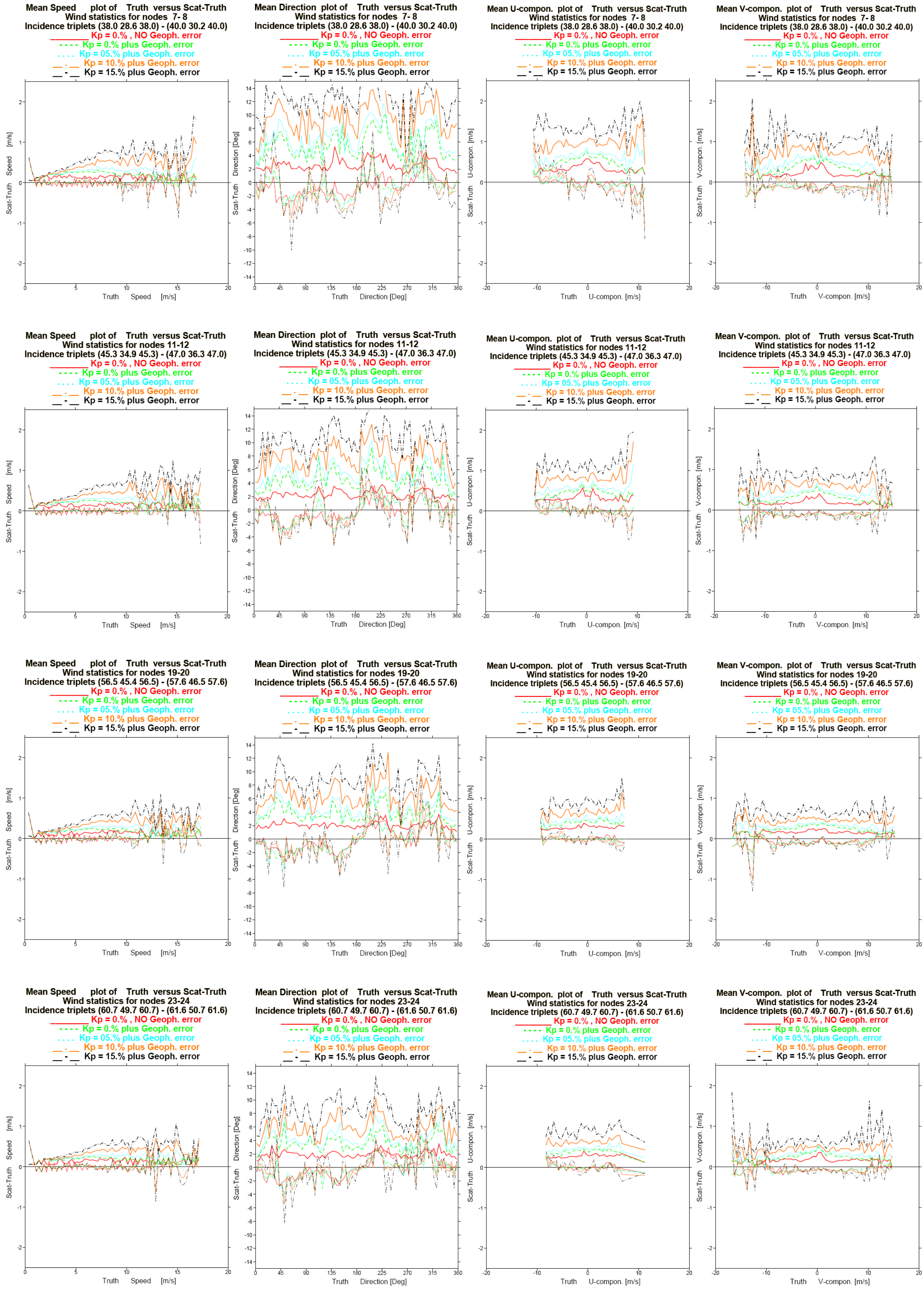

Figure 4: Bias and SDE as a function of true wind speed, wind direction and wind components.

Figure 5 shows a density contoured scatter plot of the departures of the noisy winds from the truth versus truth, for wind speed, direction, and components for nodes 7 and 8 at the inner ASCAT swath for Kp = 5%. The plots show behaviour typical of inner swath nodes. It is noted that the wind speed departures are well behaved and no anomalously large departures exist. This is markedly different for wind direction, where at some particular directions anomalously large positive or negative departures seem more likely than at other directions. From the component scatter plots we can see that these points are likely to be at low wind speed, since some large departure values exist at low component speeds, and since the SDE is larger for low component values than for higher ones while the speed SDE is more constant versus speed. The strong curvature (non-linearity) of the cone surface at low wind speeds and varying direction may be the cause. However, the number of anomalous points is not very large.

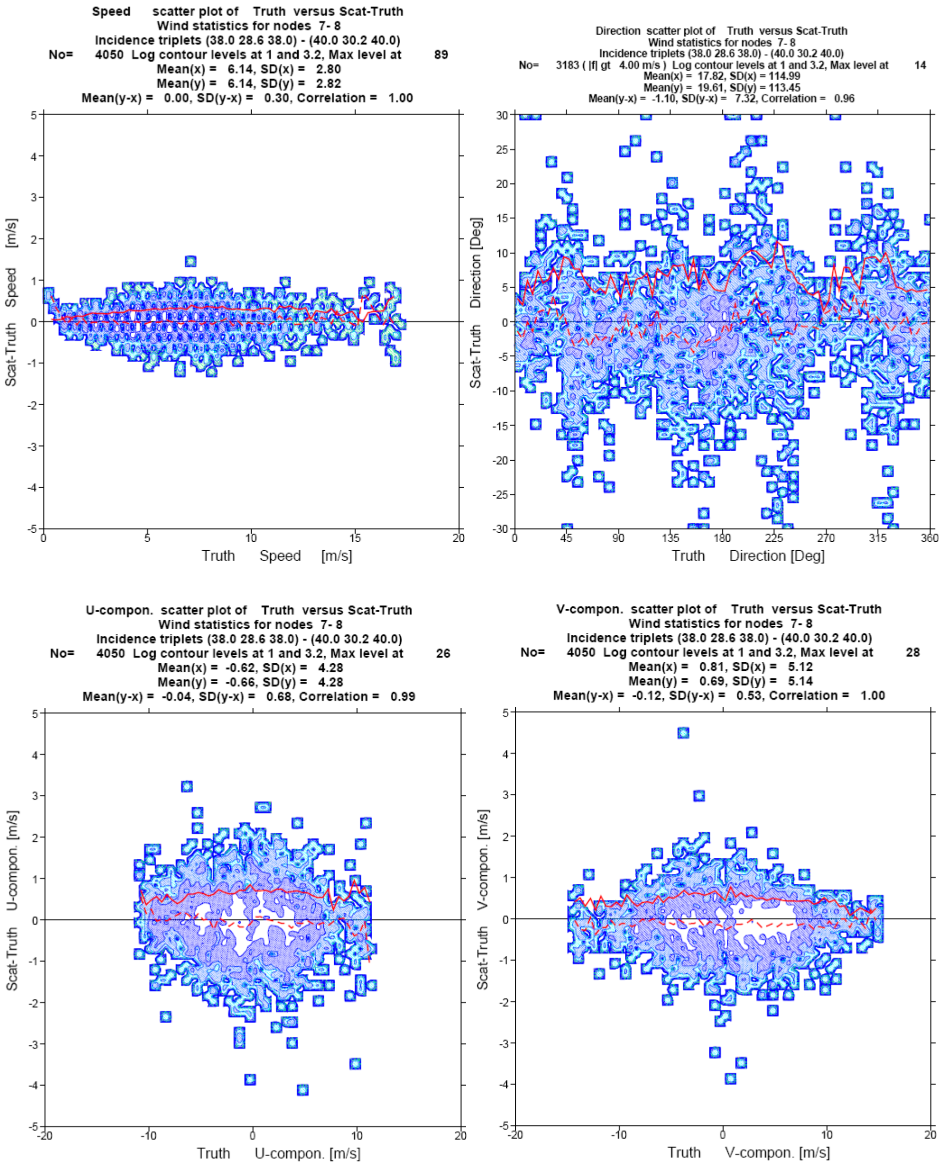

Figure 5: Departures of the noisy winds from the truth versus truth for nodes 7-8 and Kp = 5%.

Figure 6 is similar to Figure 5, but here nodes 23 and 24 are plotted for Kp = 10%. I note that Figure 6 looks very similar to Figure 5, except that the number of anomalous points for low wind speeds seems to be somewhat less at the outer swath. Scatter plots were made for all the nodes and scenarii shown in Figure 4, but Figures 5 and 6 capture nicely the general behaviour.

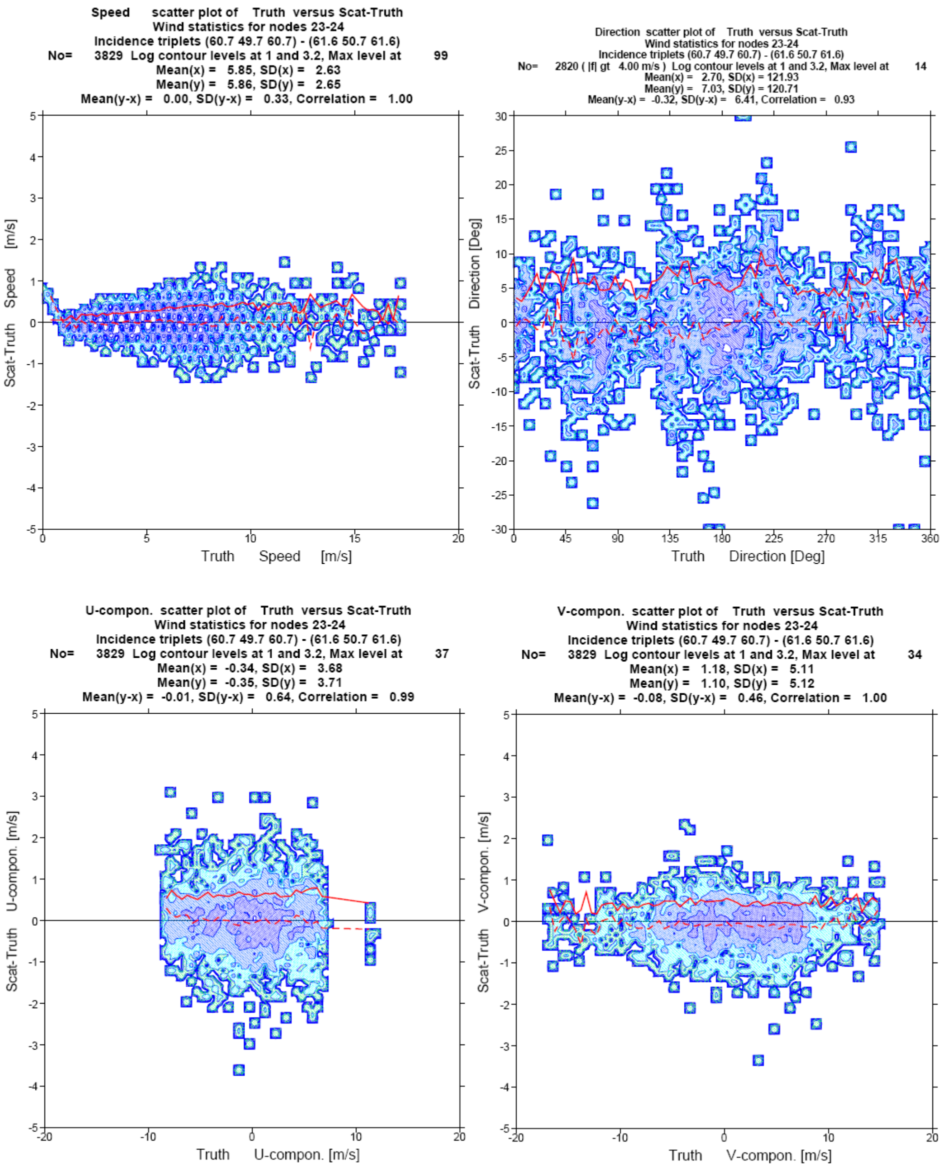

Figure 6: See Figure 5, but for nodes 23-24 and Kp = 10%

Conclusions

From Figures 3-6 it becomes clear that one may allow more instrument noise at the outer swath than at the inner. For example, from Figure 3, if one were to take Kp = 5% at nodes 7 and 8 as a reference performance, than one might allow Kp = 10% at the outer swath. Given the user requirements, Figure 3 can thus be used for setting up the radiometric resolution requirements for the ASCAT instrument. The behaviour as a function of wind direction seems the most problematic because of anomalies. However, the anomalies occur at low wind speed, such that the uncertainty in the wind vector is often not so large. The number of anomalous points increases with Kp, but these points seem to be more prevalent at the inner swath. I suggest that the statistics shown in Figures 5 and 6 are acceptable as a performance reference. When Kp = 5% for a footprint of 50 km, then Kp = 10% for a footprint of 25 km, if one were to take the Signal-to-Noise-Ratio proportional to the square root of the area sensed. Now, for nodes 7 and 8 the mean squared vector error is 0.8 and 1.6 m^2s^{-2} for Kp = 5% and Kp = 10% respectively. The difference of 0.8 m^2s^{-2} may be compared against the variability that one typically expects on scales between 25 and 50 km. Stoffelen and Anderson [4] use a climatological wind vector spectrum for this: $E = 0.0024\ (2\ p\ /l\ )^{-5/3}$ where E is the wind vector variance density spectrum in $m^3\ s^{-2}$. Integration of this spectrum over wavelength l from 0 to 25 km and 0 to 50 km, and subtracting both wind vector variabilities, gives a wind vector variability on scales between 25 and 50 km of approximately 0.8 m^2s^{-2}. This is equal to the expected SDE increase when reducing the footprint. In practice this will mean that the potential gain in resolution is blurred by the decreased performance of the instrument. From the above, it may be clear that when 25 km resolution data is required, that then, generally speaking, Kp should be better than the values used for Figures 5 and 6. However, we note that in particular cases (meteorological instability, tropical cyclones) the variability in the wind may be considerably larger than that predicted by a general wind spectrum as defined above. It is obvious that in those cases, a valuable gain in performance is achieved by processing at the 25 km resolution with the radiometric resolution being used here.

References

[1] Stoffelen, Ad and David Anderson, "Scatterometer Data Interpretation: I. Measurement Space and inversion", J. Atm. and Ocean Techn., in press, 1997.

[2] Stoffelen, Ad and David Anderson, "Scatterometer Data Interpretation: II. Transfer Function Estimation and Validation", J. Geoph. Res. (C), in press, 1997.

[3] Stoffelen, A.C.M. and D.L.T. Anderson, "Wind retrieval and ERS-1 radar backscatter measurements", Adv. Space Res. 13 (5), pp. (5)53-(5)60, 1993.

[4] Stoffelen, Ad and David Anderson, "The ECMWF contribution to the characterisation, interpretation, calibration and validation of ERS-1 scatterometer backscatter measurements and winds, and their use in numerical weather prediction. ESA study contract number: 9097/90/NL/BI published by ECMWF, Shinfield Park, Reading, UK, February 1995.